HHS Public Access

Author manuscript

J Steroid Biochem Mol Biol. Author manuscript; available in PMC 2017 November 01.

Published in final edited form as:

J Steroid Biochem Mol Biol. 2016 November ; 164: 258–264. doi:10.1016/j.jsbmb.2015.09.001.

Selective Regulation of *Mmp13* by 1,25(OH)$_2$D$_3$, PTH, and Osterix through Distal Enhancers

Mark B. Meyer[*], **Nancy A. Benkusky**, **Melda Onal**, and **J. Wesley Pike**

University of Wisconsin at Madison, Madison, WI 53706 USA

Abstract

Matrix metalloproteinase 13 (MMP13, collagenase-3) is a vital component for chondrocyte and osteoblast maturation, and is aberrantly expressed in numerous disease states. At the transcriptional level, *mmp13* is controlled by many different growth factors and hormones. Most notably, *mmp13* is regulated by the vitamin D hormone (1,25(OH)$_2$D$_3$), parathyroid hormone (PTH), and several cytokines. These activities occur through participation by the transcription factors VDR, RUNX2, FOS, JUN, and Osterix (OSX), respectively. Recently, we discovered that *mmp13* is regulated by elements quite distal to the transcriptional start site −10, −20, and −30 kb upstream. These enhancers, along with minor contributions from the region proximal to the promoter, are responsible for the ligand inducible and, most strikingly, the basal activities of *mmp13* gene regulation. Here, we found that the actions of PTH and OSX do not occur through the −10 kb VDR bound enhancer. Rather, the −30 kb RUNX2 bound enhancer and the promoter proximal regions were essential for activity. Through RUNX2 deletion and OSX overexpression in cells, we showed a specific role for OSX in *mmp13* regulation. Finally, we created an *in vivo* CRISPR deleted −10 kb enhancer mouse model. Despite normal bone density and growth, they fail to up-regulate *mmp13* in response to 1,25(OH)$_2$D$_3$. These data are consistent with those obtained through UAMS osteoblast cell culture and further define the specific roles of distal enhancers in the regulation of *mmp13*.

Keywords

ChIP-seq; *mmp13*; VDR; PTH; histone modification; Osterix; Sp7; RUNX2; vitamin D; 1,25(OH)$_2$D$_3$

1 Introduction

MMP13 (collagenase-3, Mmp-13) serves to degrade extracellular collagens during the remodeling process in maturing chondrocytes and osteoblasts [1, 2]. The aberrant expression of *Mmp13,* often along with increases in RUNX2 expression, has deleterious consequences

[*]Correspondence to: Department of Biochemistry, University of Wisconsin-Madison, Hector F. Deluca Biochemistry Laboratories, Room 545, 433 Babcock Drive, Madison, WI 53706. Tel.: (608) 262-8230; Fax: (608) 263-7609. mmeyer@biochem.wisc.edu.

in cancers such as chondrosarcomas, breast and lung as well as disease progression in atherosclerosis and osteoarthritis [3-6]. *mmp13* expression is regulated by many different growth factors, cytokines, and hormones such as the vitamin D hormone ($1,25(OH)_2D_3$), the parathyroid hormone (PTH), IL-1β, TNFα, estrogens, BMP2 and others [7-11], all of which are postulated to interact with several transcriptional elements near the promoter of *mmp13*. Recently, we investigated *mmp13* through ChIP-seq analyses and discovered that it was controlled by three distinct enhancers located at −10 kb, −20 kb, and −30 kb upstream of the transcriptional start site (TSS) of the *mmp13* gene [12-14]. Utilizing CRISPR/Cas9 genomic deletion methods to delete each of these three regions, we found that the −10 kb enhancer was responsible for $1,25(OH)_2D_3$-induced activity. As a consequence of deletion, the basal expression of the gene was slightly reduced; however a sharp dose- and time-dependent repression of *mmp13* by $1,25(OH)_2D_3$ then became evident. The −30 kb enhancer, on the other hand, was found to be the major site of RUNX2 binding at the genomic locus and with its deletion, the basal expression of the gene was almost completely eliminated. The activities of the gene were only modestly altered following deletion of a promoter proximal fragment (−454 to −98bp) with only minor basal decreases and no effect on $1,25(OH)_2D_3$ induction. These studies define a more comprehensive mechanism of distal basal and $1,25(OH)_2D_3$- induced regulation for *mmp13*.

Our previous studies of the *mmp13* regulatory mechanism were conducted in UAMS cells, a mouse model of osteoblast differentiation [12]. In this report, we examined further the contributions of PTH to the expression of *mmp13* using our previously generated enhancer deletion cell lines. We found that PTH did not utilize the −10 kb enhancer for its activity; rather it employed the promoter proximal and the −30 kb regions. We also found that OSX was specifically recruited to the −30 kb, −20 kb and promoter proximal regions, but not to the −10 kb enhancer, to activate *mmp13* expression. This identified the −30 kb RUNX2 responsive enhancer as important for OSX activity, which may indicate an interaction of at least two factors at this enhancer. Finally, we have begun to establish a comparable *in vivo* mouse models to validate and extend these cell based results using the same CRISPR methods recently described [12]. Herein, we present results of the first of these models in the −10 kb enhancer deletion. These mice have a normal growth and bone phenotype with the exception that they are unable to up-regulate *mmp13* in bone cells when challenged with $1,25(OH)_2D_3$ *ex vivo*. We will continue to phenotype this model for activation by alternative compounds and growth factors. Overall, these studies further our understanding of the distal regulation of *mmp13* modulation in the mouse.

2 Materials and Methods

2.1 Reagents and Cell Culture

All reagents and antibodies were obtained as previously published unless otherwise noted [12, 13]. Parathyroid Hormone (PTH, 1-84 human) was obtained from Bachem (#H-1370.0100 Torrence, CA). Osterix (Sp7) antibody for western blot and ChIP was obtained from Abcam (#ab22552 Cambridge, UK). FLAG mouse monoclonal Anti-FLAG M2-HRP for western blot was from Sigma-Aldrich (#A8592) and rabbit polyclonal Anti-FLAG for ChIP assay from Thermo-Fisher (#PA1-984B). Traditional genotyping PCR was

completed with GoTaq (Promega) and all real-time qPCR was completed with the StepOnePlus (Life Technologies) using TaqMan for gene expression assays (Life Technologies) and Faststart Universal SYBR Green Mastermix for ChIP (Roche). All primers and TaqMan assays used are available on the Pike Lab website (http://www.pikelab.org). UAMS osteoblastic cells were cultured as recently reported [12].

2.2 Cloning and Lentiviral Overexpression of Osterix

Osterix lentiviral overexpression plasmids (pLeGO-OSX and pLeGO-3xFLAG-OSX) were made through Gibson Isothermal Assembly as recently described for RUNX2 overexpression [12]. Briefly, mouse OSX/Sp7 from pCMV-FLAG-Sp7 [15] was combined in a PCR reaction with primers that contained homologous sequence to the pLeGO plasmid with or without a 3xFLAG sequence. pLeGO-OSX forward primer 5'-GTCCTCCGATTGACTGAGTCGCCCGGATCCATGGCGTCCTCTCTGCTTGAGGAAGAAGC, pLeGO-3xFLAG-OSX forward primer 5'-GATTGACTGAGTCGCCCGGATCCATGGACTATAAGGACCACGACGGAGACTACAAGGA TCATGATATTGATTACAAAGACGATGACGATAAGATGGCGTCCTCTCTGCTTGAGGAAG AAG , and a common reverse primer 5'-ACGAAGTTATTAGGTCCCTCGACGAATTCTCAGATCTCTAGCAGGTTGCTCTGCTCTGG. Resulting clones were sequenced for verification of appropriate OSX insertion and confirmed by western blot for appropriate size and expression. Lentiviral packaging, infection, and expression of pLeGO-OSX and pLeGO-3xFLAG-OSX was completed as recently described [12].

2.3 Chromatin Immunoprecipitation Assay (ChIP)

Chromatin Immunoprecipitation (ChIP) was performed as recently described [13, 14] using antibodies listed in Reagents (2.1).

2.4 CRISPR Generated Mice

CRISPR plasmids were created as recently described [12]. All animal protocols were reviewed and approved by the University of Wisconsin – Madison Institutional Animal Care and Use Committee. CRISPR mice were generated at the University of Wisconsin Biotechnology Center Transgenic Animal Facility. For CRISPR mouse injections, RNA guides were created through T7-*in vitro* translation via T7 MEGAshortscript (Life Technologies) kit [16] after constructing a PCR template with the additional T7 sequence (5'-TTAATACGACTCACTATAGG-) appended to the 5' end of the guide sequence. Guide 1 5'-TTAATACGACTCACTATAGGGAGATGCCCTGTGAAGCTCA and guide 2 5'-TAATACGACTCACTATAGGGTCTTCAGGATAGAACACTC paired with reverse primer: 5'-CAAAAAAGCACCGACTCGGTGCCACTTTTTCAAG from pX330 or pX458 plasmids [17] harboring the guide 1 and 2 sequences shown above. 50ng/μL of RNA guide for both guides were combined with 40ng/μL of Cas9 protein (PNA Bio) into Embryomax injection buffer (Millipore). The solution was injected into the pronucleus of one day fertilized embryos isolated from hyperovulating female FVB mice as described previously [18] and implanted into recipient females. Resulting pups were tail clipped, DNA isolated (Red Extract and Amp, Sigma) and genotyped with spanning primers followed by

sequencing. Heterozygous founder mice were identified (~30%) and crossed until the appropriate homozygous knockout and wildtype littermates were obtained for study.

2.5 Tissue Extraction, RNA isolation, RT-qPCR

Primary bone marrow cells (pBMCs) were obtained by flushing the marrow from femur shafts from 2 month old CRISPR mice and their wildtype litter mates as recently described [19]. The cells were then cultured for 8-10 days, renewing one half of the media every 2 days until assay. Cells were treated for 6 or 24 h with the indicated factors and 1 μg of isolated total RNA was reverse transcribed using the High Capacity cDNA Kit (ABI, Foster City, CA), and then diluted to 100 μL with RNAse/DNAse I free water. qPCR was performed using primers specific to a select set of genes by TaqMan analyses.

3 Results and Discussion

3.1 Up-regulation of *mmp13* expression by PTH is mediated via the promoter proximal region of the gene

The effects of PTH on the expression of *mmp13* have been studied for the past decade [9, 20-22] and PTH is an important regulator of bone quality and growth [23, 24]. These studies have been focused on the promoter proximal region of *mmp13*. With the recent revelation that RUNX2 and VDR are acting at distal enhancers [12], we utilized our *mmp13* CRISPR enhancer deletion cell lines to study PTH activation. The deletion daughter cells were created in the UAMS osteoblastic cell line and these cells stably express the human PTH receptor [12]. Wildtype and deletion daughter cell lines were treated with vehicle, 100 nM PTH or 1 μM forskolin (FSK, a PTH mimetic that stimulates cAMP and PKA pathway). As can be seen in Fig. 1, the raw relative quantitation (RQ) levels for *mmp13* (A), *Vdr* (B), and *RankL* (C) are reported in response to PTH and FSK at 3 and 24 hours. The experimental wildtype (E/WT, cells that were clonally isolated through CRISPR process but found to be of wildtype sequence) exhibited a 2 to 3 fold increase in *mmp13* expression with both PTH and FSK at 24 hours. The −10k enhancer deleted cells (−10k KO) showed a profile similar to that of E/WT cells. Despite the extreme loss of basal activity, the −30 kb enhancer deleted cells (−30k KO) increased sensitivity to PTH to 9-fold; however, overall levels compared to E/WT cells remained low (expanded scale shown right). Interestingly, deletion of the region proximal to the promoter (PP KO) had a significant inhibitory effect on the inducibility of *mmp13* in response to PTH, reducing the fold change to less than 1.5. The PP KO cells also had a lower basal activity of *mmp13* expression than the E/WT samples. The VDR KO cells had a lower basal activity and an impaired induction as well. Finally, global deletion of RUNX2 (RUNX2 KO) in the cells showed that induction with PTH requires RUNX2, as previously reported (expanded scale shown right) [9, 20, 21]. The expression of the control genes, *Vdr* and *RankL* was impaired as expected only when VDR or RUNX2 was deleted, but not when the specific *mmp13* enhancers were deleted. It is important to note that the *Vdr* transcript remains detectable by TaqMan qPCR despite the CRISPR partial deletion of exon 3 in the “VDR KO” cells, so *Vdr* gene regulation can still be studied in absence of the VDR protein [12].

These studies with PTH induction demonstrate that the enhancer responsible for the VDR activity (−10 kb) is dispensable for PTH activities. We also found that while deletion of either the RUNX2 enriched enhancer (−30 kb) or RUNX2 completely crippled the basal expression of *mmp13*, PTH induction could still be observed even with a loss in basal activities. However, loss of RUNX2 binding at the promoter proximal region (−454 to −98bp, which eliminated RUNX2 binding sites, but not an apparent AP-1 site [25]) had limited effects on the activities of PTH. Therefore, these RUNX2-boundenhancers likely function in synergy for the modulation of *mmp13* by PTH. The effects of global deletion of the VDR on PTH induction of *mmp13* is less clear. Perhaps VDR interaction with RUNX2 and the effects $1,25(OH)_2D_3$ to down-regulate RUNX2 expression may be vital to this pathway. Thus, the induction of *mmp13* by PTH, although not as robust a response as that seen with $1,25(OH)_2D_3$, involves at least two distinct enhancers, but not the $1,25(OH)_2D_3$-inducible −10 kb enhancer, for its full activation.

3.2 Osterix (OSX) binds to upstream enhancers to up-regulate *mmp13* expression

Mice without OSX are devoid of bone and the activity of the protein relies on the presence and expression of RUNX2 [26]. It was recently demonstrated that *mmp13* activity was modulated via increasing concentrations of exogenously transfected Osterix on an *mmp13* promoter reporter [27]. It is unclear if RUNX2 and OSX binding is coordinated to help control genes such as *mmp13* that are important to bone. As in the studies of PTH activity, we were interested in whether OSX bound at the *mmp13* locus and whether OSX utilized the same enhancers as RUNX2 (and/or VDR) for induction of *mmp13*. To explore the activities of OSX in the UAMS cell line, we created a lentiviral overexpression system for OSX which introduced a 3xFLAG tag to the N-terminus. This system allowed the overexpression of OSX in WT cells, its re-introduction following potential CRISPR deletion of OSX and re-expression in the RUNX2 KO cells (which have low levels of OSX expression [12]). The FLAG tag together with a FLAG-specific antibody also allows better signal to noise ratios in ChIP and ChIP-seq experiments. The lentiviral OSX and lentiviral 3xFLAG-OSX were infected, along with the parental control empty pLeGO-G plasmid, into WT and RUNX2 KO cells for 72 hours, protein was isolated, and a western blot was completed with antibodies for OSX, FLAG, and βTUBULIN. As can be seen in Fig. 2A, OSX was detectable in WT cells and its levels were increased significantly with the OSX lentivirus and further still with the FLAG-OSX lentivirus. Interestingly, since OSX can regulate its own cognate gene, *Sp7*, increased FLAG-OSX levels were accompanied by an elevation in levels of the wildtype-size OSX in addition to FLAG-OSX (slightly larger). In RUNX2 KO cells, endogenous OSX protein was not detected which is a known consequence of the loss of RUNX2 [12, 26]. In these cells, a lentiviral overexpression system for RUNX2 [12] was used instead of the OSX (no FLAG) virus to demonstrate that RUNX2 can up-regulate OSX. In fact, the levels of OSX are increased with re-expression of RUNX2 in the RUNX2 KO cells. In Fig. 2A (far right), the FLAG-OSX again increased the levels of wildtype OSX as well as the FLAG-OSX in the RUNX2 KO cells as was seen in the WT cells as well. Therefore, the OSX lentiviral constructs appropriately overexpress the OSX protein.

To determine if the OSX protein was functional in gene expression and specifically in *mmp13* regulation, UAMS wildtype and RUNX2 KO cells transduced with the control virus, OSX virus (OSX), or the FLAG-OSX virus (FLAG-OSX) were infected for 72 h, then treated with vehicle or 100nM $1,25(OH)_2D_3$ for 24 h. Gene expression was tested for *mmp13*, *Sp7* and *RankL*. Overexpression of OSX increased basal expression of *mmp13* (Fig. 2B), however the response to $1,25(OH)_2D_3$ was not increased. This may be due to the down-regulatory effect of $1,25(OH)_2D_3$ on the *Sp7* gene (Fig. 2C). In Fig. 2B, RUNX2 KO cells showed a low basal level of *mmp13*. Viral introduction of either OSX or FLAG-OSX increased *mmp13* basal levels. (The scale of Fig. 2B has been expanded on the right). Although expression remains low, the regulation of *mmp13* by OSX is present and statistically significant. In Fig. 2C, the basal levels of *Sp7* are increased with introduction of OSX and FLAG-OSX, despite being greatly inhibited by $1,25(OH)_2D_3$. Again, the basal levels of *Sp7* in the RUNX2 KO cells were low, although introduction of OSX increased the transcript expression of *Sp7* (Fig. 2A). Finally, *RankL* was not affected by the overexpression of OSX. These data indicate that the lentiviral overexpressed OSX protein is functional and contributes to the regulation of *mmp13*.

The RUNX2 KO cells did not differentiate or mineralize due, in part, to lack of OSX expression [12, 26]. We tested the RUNX2 KO cells for their ability to differentiate into mature mineralizing osteoblasts by overexpressing OSX. Despite the elevated levels of OSX in these cells, they remained unable to properly differentiate or mineralize, as calcium content assay readings were undetectable and alizarin red staining was unchanged from day 0 cells (data not shown). Therefore, re-/over-expression of OSX alone was insufficient to rescue this phenotype, suggesting that RUNX2 has more diverse actions in differentiation than simply controlling OSX expression.

To determine how OSX affected transcription, we examined the binding of OSX by direct ChIP qPCR assay. As in Fig. 2B, WT and RUNX2 cells were infected with control virus or FLAG-OSX (F-OSX) for 72 h. Following this infection, cells were collected for ChIP, immunoprecipitated with antibodies for OSX, FLAG, and control IgG, and then examined with primers designed to amplify the *mmp13* locus at −30 kb, −20 kb, −10 kb, and the promoter proximal region (Pro Prox) (Fig. 2E). For each region, the WT control (grey) was compared to the WT + FLAG-OSX (black) and the RUNX2 KO control (red) was compared to the RUNX2 KO + FLAG-OSX (green). At the −30 kb enhancer, there was a high level of OSX binding following OSX immunoprecipitation. Binding was not enhanced due to overexpression of FLAG-OSX. RUNX2 KO cells, which have very low OSX levels, show no OSX binding at the −30 kb enhancer unless FLAG-OSX is introduced. Therefore, this interaction appears specific for OSX at the −30 kb enhancer. The FLAG immunoprecipitation demonstrates this specificity further and shows that FLAG-OSX was recruited to the −30 kb enhancer. The IgG control immunoprecipitation sets a threshold for signals and was very low in these samples. OSX was also specifically recruited to the −20 kb and promoter proximal region. In both regions, overexpression of FLAG-OSX increased the binding of OSX in WT cells and the FLAG specific or RUNX2 KO cells corroborate these data. OSX binding at the −10 kb enhancer was not significantly enriched compared to IgG and the FLAG specific ChIP was not enriched over background. Thus, it would appear that the only region that is not involved in OSX binding is the −10 kb enhancer. The binding

activities of OSX at *mmp13* are compared to those at known *Vdr* gene enhancers [28], which were also increased through overexpression of FLAG-OSX. Taken together, these data indicate that OSX is an activator of *mmp13* expression. These activities clearly occur at the previously indicated promoter proximal region [27] as well as at the upstream identified enhancers [12]. Moreover, overexpressed OSX protein was functional and provides an excellent reagent with which to test the activities of OSX across the genome.

3.3 *In vivo* enhancer deletion in mice reveals the loss of *mmp13* induction

Combining our entire datasets [12], we have gained a more complete picture of *mmp13* regulation in the UAMS osteoblastic cells. To validate these data, however, we turned to an examination of the enhancer deletions in the *mmp13* locus *in vivo*. We are currently developing mouse models for the −10 kb, −30 kb and promoter proximal enhancer deletions, along with a full *mmp13* gene knockout for comparison. To begin, we first deleted the −10 kb region in the mouse as this enhancer is responsible for the VDR-mediated $1,25(OH)_2D_3$-induced activities. Accordingly, CRISPR/Cas9 machinery was used to create a germline −10 kb *mmp13* enhancer deleted mouse through non-homologous end joining as outlined in Materials and Methods and as recently described [12]. Two CRISPR RNA guides were created flanking the −10 kb enhancer [12] and these plasmids were used as PCR templates to append a T7 promoting sequence to the RNA guide sequence. The resulting 105 bp PCR product was then used as the template for *in vitro* transcription of the CRISPR RNA guides. These RNA guides were combined with Cas9 protein for embryo injection. This method provides the cell with the complete and degradable gene-editing machinery without leaving residual DNA plasmids that may incorporate into the recipient genome inherent to traditional mouse knockouts. The resulting founder mice (heterozygous, ~30% efficiency) were then crossed to obtain appropriate homozygous knockout and wildtype numbers for experimentation.

Homozygous −10 kb deleted mice were initially phenotyped relative to their wildtype littermates for potential bone mineral density (BMD) changes and by using *ex vivo* $1,25(OH)_2D_3$ treated primary bone marrow cultures at 2 months of age. Global *mmp13* gene knockout mice display aberrant bone development embryonically, and exhibit a growth phenotype comprised of lower BMD, remodeling defects of mid-cortical bone, and lower bone quality through loss of *mmp13*-mediated remodeling in mice of 4-8 weeks [29, 30]. However, in the −10 kb KO mice there was no change in either total body, femur, or spine BMD (data not shown) at 8 weeks of age and no change was noted in the growth or bone length at 4 and 5 weeks of age (data not shown) as was reported in complete *mmp13* gene knockout mice. Therefore, these mice appeared to have a normal developmental and skeletal phenotype. Additional parameters of growth and development will be assessed in conjunction with the −30 kb and promoter proximal knockout mice.

Changes in the regulation of *mmp13* were observed in *ex vivo* studies, however (Fig. 3). Primary bone marrow cells (pBMCs) were cultured from the femur shafts of male and female wildtype (WT) or −10 kb enhancer knockout mice (−10k KO) (n=3 each group) for 8 days which lead to an enrichment of the adherent osteoblast population. The cells were then treated with ethanol vehicle or 100nM $1,25(OH)_2D_3$ for 6 and 24 hours. As can be seen in

Fig. 3, changes in basal and 1,25$(OH)_2D_3$ induced gene expression for *mmp13* (A), *Vdr* (B), and *RankL* (C) were detected. There was an increase of *mmp13* expression in both female and male WT mice, with a higher basal level seen in male versus female mice, which could potentially be due to involvement of estrogens [10, 31]. Interestingly, however, cells from the −10k KO mice were no longer induced by 1,25$(OH)_2D_3$, but rather were now repressed by 1,25$(OH)_2D_3$, recapitulating the observations made in the cell culture model [12]. Repression by 1,25$(OH)_2D_3$ after treatment is likely caused at least, in part, by secondary interactions with RUNX2, which is down-regulated by 1,25$(OH)_2D_3$. *Vdr* and *RankL* gene expression was unchanged in the knockout mice. These data indicate that 1) the CRISPR method for enhancer deletions is a viable technique to study the roles of enhancers *in vivo* and 2) the chromatin organization and regulation of *mmp13* by 1,25$(OH)_2D_3$ in both cell culture and animal models is similar. The latter observation is important as the enhancer and regulatory structure of the *mmp13* gene in the UAMS and MC3T3-E1 cells and even in our primary marrow-derived MSC cells [12] may differ slightly from the primary cells isolated here, as cultured lines may change their chromatin structure under the stress of culture conditions. We have yet to complete ChIP-seq in these primary cells, however equivalent loss of *mmp13* regulation in our KO mice to our cell culture models indicates they may be similar. We predict that deletion of the −30 kb enhancer in mice will have a skeletal phenotype comparable to that seen in the full *mmp13* knockout mouse.

3.4 Conclusions

The activities of *mmp13* distal enhancers are far more diverse than originally thought. There are many compounds, growth factors, hormones and cytokines that can modulate their activities. The mechanisms of regulation may prove vital to disease progression that can be affected by aberrant *mmp13* expression. Here, we have shown that aside from the basal expression and regulation by 1,25$(OH)_2D_3$ we recently documented [12], these discovered enhancers are essential for the full regulatory activities of PTH and OSX. With continued development of our CRISPR enhancer knockout mouse models (−30 kb, −10 kb, and PP), and the crossing of these knockouts into genetic disease backgrounds, a better understanding of the role of *mmp13* in health and disease is likely.

Acknowledgements

We thank the Pike Lab members for their helpful discussions in preparation of this manuscript. We also thank Kathleen Krentz and the University of Wisconsin Biotechnology Center Transgenic Animal Facility for injection and generation of the CRISPR/Cas9 mice. This work was supported by National Institutes of Health grant (NIDDK) DK-072281 to J.W.P.

References

1. Inada M, Yasui T, Nomura S, Miyake S, Deguchi K, Himeno M, Sato M, Yamagiwa H, Kimura T, Yasui N, Ochi T, Endo N, Kitamura Y, Kishimoto T, Komori T. Maturational disturbance of chondrocytes in Cbfa1-deficient mice. Dev Dyn. 1999; 214(4):279–290. [PubMed: 10213384]
2. Komori T, Yagi H, Nomura S, Yamaguchi A, Sasaki K, Deguchi K, Shimizu Y, Bronson R, Gao Y, Inada M, Sato M, Okamoto R, Kitamura Y, Yoshiki S, Kishimoto T. Targeted disruption of Cbfa1 results in a complete lack of bone formation owing to maturational arrest of osteoblasts. Cell. 1997; 89(5):755–764. [PubMed: 9182763]

3. Uría JA, Balbín M, López JM, Alvarez J, Vizoso F, Takigawa M, López-Otín C. Collagenase-3 (MMP-13) expression in chondrosarcoma cells and its regulation by basic fibroblast growth factor. Am J Pathol. 1998; 153(1):91–101. [PubMed: 9665469]
4. Gao P, Yang JL, Zhao H, You JH, Hu Y. Common polymorphism in the MMP-13 gene may contribute to the risk of human cancers: a meta-analysis. Tumour Biol. 2014; 35(10):10137–10148. [PubMed: 25023404]
5. Sukhova GK, Schönbeck U, Rabkin E, Schoen FJ, Poole AR, Billinghurst RC, Libby P. Evidence for increased collagenolysis by interstitial collagenases-1 and -3 in vulnerable human atheromatous plaques. Circulation. 1999; 99(19):2503–2509. [PubMed: 10330380]
6. Mitchell PG, Magna HA, Reeves LM, Lopresti-Morrow LL, Yocum SA, Rosner PJ, Geoghegan KF, Hambor JE. Cloning, expression, and type II collagenolytic activity of matrix metalloproteinase-13 from human osteoarthritic cartilage. J Clin Invest. 1996; 97(3):761–768. [PubMed: 8609233]
7. Deguchi JO, Aikawa E, Libby P, Vachon JR, Inada M, Krane SM, Whittaker P, Aikawa M. Matrix metalloproteinase-13/collagenase-3 deletion promotes collagen accumulation and organization in mouse atherosclerotic plaques. Circulation. 2005; 112(17):2708–2715. [PubMed: 16230484]
8. Varghese S, Canalis E. Regulation of collagenase-3 by bone morphogenetic protein-2 in bone cell cultures. Endocrinology. 1997; 138(3):1035–1040. [PubMed: 9048606]
9. Selvamurugan N, Chou WY, Pearman AT, Pulumati MR, Partridge NC. Parathyroid hormone regulates the rat collagenase-3 promoter in osteoblastic cells through the cooperative interaction of the activator protein-1 site and the runt domain binding sequence. J Biol Chem. 1998; 273(17): 10647–10657. [PubMed: 9553127]
10. Achari Y, Lu T, Katzenellenbogen BS, Hart DA. Distinct roles for AF-1 and -2 of ER-alpha in regulation of MMP-13 promoter activity. Biochim Biophys Acta. 2009; 1792(3):211–220. [PubMed: 19185056]
11. Rydziel S, Delany AM, Canalis E. Insulin-like growth factor I inhibits the transcription of collagenase 3 in osteoblast cultures. J Cell Biochem. 1997; 67(2):176–183. [PubMed: 9328823]
12. Meyer MB, Benkusky NA, Pike JW. Selective Distal Enhancer Control of the Mmp13 Gene Identified through Clustered Regularly Interspaced Short Palindromic Repeat (CRISPR) Genomic Deletions. J Biol Chem. 2015; 290(17):11093–11107. [PubMed: 25773540]
13. Meyer MB, Benkusky NA, Lee CH, Pike JW. Genomic determinants of gene regulation by 1,25-dihydroxyvitamin D3 during osteoblast-lineage cell differentiation. J Biol Chem. 2014; 289(28): 19539–19554. [PubMed: 24891508]
14. Meyer MB, Benkusky NA, Pike JW. The RUNX2 cistrome in osteoblasts: characterization, down-regulation following differentiation, and relationship to gene expression. J Biol Chem. 2014; 289(23):16016–16031. [PubMed: 24764292]
15. Goto T, Matsui Y, Fernandes RJ, Hanson DA, Kubo T, Yukata K, Michigami T, Komori T, Fujita T, Yang L, Eyre DR, Yasui N. Sp1 family of transcription factors regulates the human alpha2 (XI) collagen gene (COL11A2) in Saos-2 osteoblastic cells. J Bone Miner Res. 2006; 21(5):661–673. [PubMed: 16734381]
16. Wang H, Yang H, Shivalila CS, Dawlaty MM, Cheng AW, Zhang F, Jaenisch R. One-step generation of mice carrying mutations in multiple genes by CRISPR/Cas-mediated genome engineering. Cell. 2013; 153(4):910–918. [PubMed: 23643243]
17. Cong L, Ran FA, Cox D, Lin S, Barretto R, Habib N, Hsu PD, Wu X, Jiang W, Marraffini LA, Zhang F. Multiplex genome engineering using CRISPR/Cas systems. Science. 2013; 339(6121): 819–823. [PubMed: 23287718]
18. Meyer M, de Angelis MH, Wurst W, Kühn R. Gene targeting by homologous recombination in mouse zygotes mediated by zinc-finger nucleases. Proc Natl Acad Sci U S A. 2010; 107(34): 15022–15026. [PubMed: 20686113]
19. Galli C, Zella L, Fretz J, Fu Q, Pike J, Weinstein R, Manolagas S, O'Brien C. Targeted deletion of a distant transcriptional enhancer of the receptor activator of nuclear factor-kappaB ligand gene reduces bone remodeling and increases bone mass. Endocrinology. 2008; 149(1):146–153. [PubMed: 17932217]

20. Shimizu E, Nakatani T, He Z, Partridge NC. Parathyroid hormone regulates histone deacetylase (HDAC) 4 through protein kinase A-mediated phosphorylation and dephosphorylation in osteoblastic cells. J Biol Chem. 2014; 289(31):21340–21350. [PubMed: 24904057]
21. Lee M, Partridge NC. Parathyroid hormone activation of matrix metalloproteinase-13 transcription requires the histone acetyltransferase activity of p300 and PCAF and p300-dependent acetylation of PCAF. J Biol Chem. 2010; 285(49):38014–38022. [PubMed: 20870727]
22. Lee M, Partridge N. Parathyroid hormone signaling in bone and kidney. Curr Opin Nephrol Hypertens. 2009; 18(4):298–302. [PubMed: 19395963]
23. Mosekilde L, Søgaard CH, Danielsen CC, Tørring O. The anabolic effects of human parathyroid hormone (hPTH) on rat vertebral body mass are also reflected in the quality of bone, assessed by biomechanical testing: a comparison study between hPTH-(1-34) and hPTH-(1-84). Endocrinology. 1991; 129(1):421–428. [PubMed: 2055197]
24. Raggatt LJ, Partridge NC. Cellular and molecular mechanisms of bone remodeling. J Biol Chem. 2010; 285(33):25103–25108. [PubMed: 20501658]
25. Mengshol JA, Vincenti MP, Brinckerhoff CE. IL-1 induces collagenase-3 (MMP-13) promoter activity in stably transfected chondrocytic cells: requirement for Runx-2 and activation by p38 MAPK and JNK pathways. Nucleic Acids Res. 2001; 29(21):4361–4372. [PubMed: 11691923]
26. Nakashima K, Zhou X, Kunkel G, Zhang Z, Deng JM, Behringer RR, de Crombrugghe B. The novel zinc finger-containing transcription factor osterix is required for osteoblast differentiation and bone formation. Cell. 2002; 108(1):17–29. [PubMed: 11792318]
27. Zhang C, Tang W, Li Y. Matrix metalloproteinase 13 (MMP13) is a direct target of osteoblast-specific transcription factor osterix (Osx) in osteoblasts. PLoS One. 2012; 7(11):e50525. [PubMed: 23185634]
28. Zella LA, Kim S, Shevde NK, Pike JW. Enhancers located within two introns of the vitamin D receptor gene mediate transcriptional autoregulation by 1,25-dihydroxyvitamin D3. Mol Endocrinol. 2006; 20(6):1231–1247. [PubMed: 16497728]
29. Tang SY, Herber RP, Ho SP, Alliston T. Matrix metalloproteinase-13 is required for osteocytic perilacunar remodeling and maintains bone fracture resistance. J Bone Miner Res. 2012; 27(9): 1936–1950. [PubMed: 22549931]
30. Inada M, Wang Y, Byrne MH, Rahman MU, Miyaura C, López-Otín C, Krane SM. Critical roles for collagenase-3 (Mmp13) in development of growth plate cartilage and in endochondral ossification. Proc Natl Acad Sci U S A. 2004; 101(49):17192–17197. [PubMed: 15563592]
31. Schiltz C, Marty C, de Vernejoul MC, Geoffroy V. Inhibition of osteoblastic metalloproteinases in mice prevents bone loss induced by oestrogen deficiency. J Cell Biochem. 2008; 104(5):1803–1817. [PubMed: 18384129]

Highlights

- *mmp13* is regulated by coordination of three distinct distal enhancers at −10, −20, and −30 kb.
- PTH utilizes the promoter proximal region for activation of *mmp13*.
- Osterix binds to and regulates *mmp13* through the −30 kb, −20 kb and promoter proximal regions.
- CRISPR deletion of the −10 kb enhancer in mice leads to a loss of *mmp13* induction by $1,25(OH)_2D_3$.

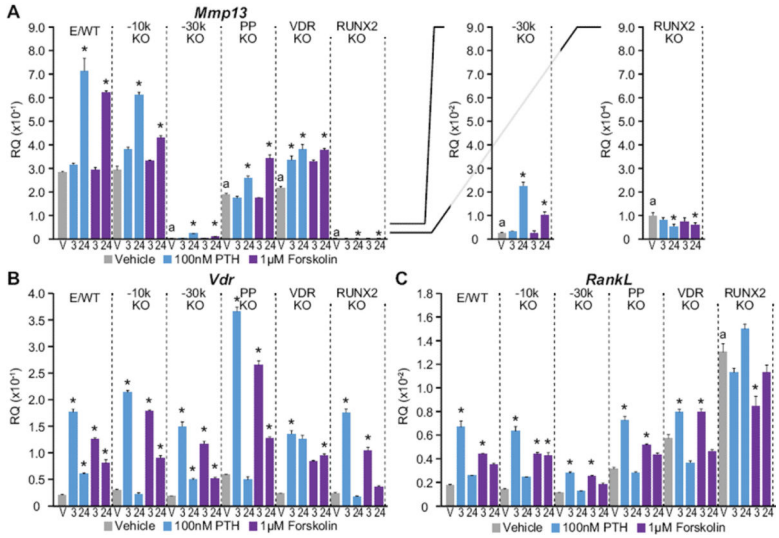

Figure 1.

Up-regulation of *mmp13* expression by PTH is mediated through the promoter proximal region of its gene. CRISPR-deleted and clonally isolated UAMS cell lines for experimental wildtype (E/WT), −10 kb region deletion (−10k KO), −30 kb region (−30k KO), Promoter Proximal (PP KO), VDR deletion (VDR KO), and RUNX2 deletion (RUNX2 KO) were treated with vehicle (grey) or PTH (100 nM, blue) or Forskolin (FSK, 1 μM, purple) for 3 and 24 h prior to RNA isolation, reverse transcription, and TaqMan qPCR analysis for *mmp13* (A), *Vdr* (B), and *RankL* (C). Expanded scales are shown on the right for −30 k KO and RUNX2 KO cell lines of A (note scale change). Data are displayed as Relative Quantitation (RQ) normalized to *Gapdh* in a triplicate set of assays ± SEM. *, $p<0.05$ 24 or 3 h versus 0 h within cell type by Student's t-test. a, $p<0.05$ basal vehicle of each line versus E/WT by Student's t-test.

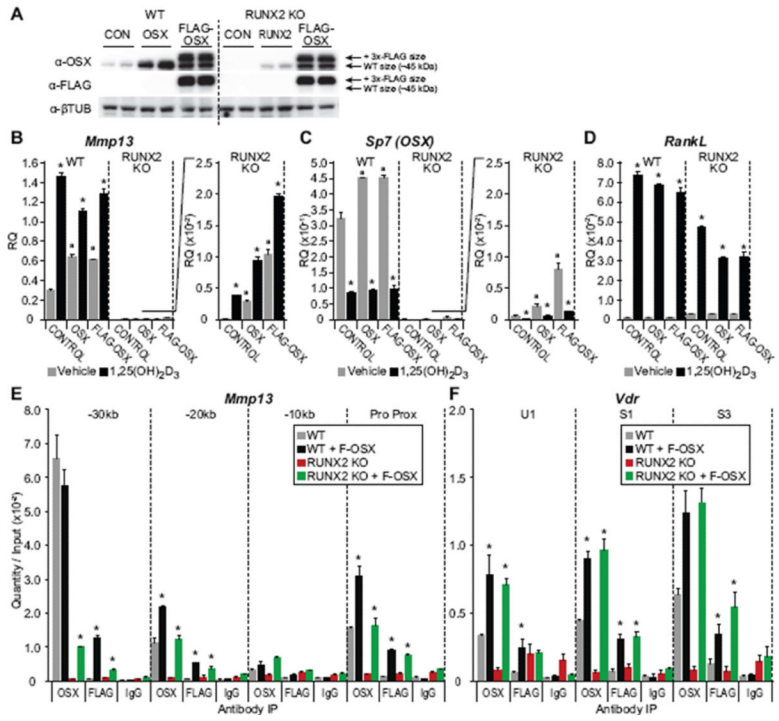

Figure 2.

Osterix binds to the upstream enhancers to up-regulate *mmp13* expression. A, western blot analysis with OSX and FLAG antibodies in WT (UAMS) or RUNX2 KO cells infected with either lentivirus for pLeGO-G (control, CON), pLeGO-OSX (OSX), or pLeGO-3xFLAG-OSX (FLAG-OSX). The RUNX2 KO cells were also infected with pLeGO-RUNX2-2A-GFP. All samples are displayed in duplicated and normalized to to β-TUBULIN levels. B, WT (UAMS) or RUNX2 KO cells infected with Control, OSX, or 3xFLAG-OSX were treated with vehicle (grey) or 100 nM $1,25(OH)_2D_3$ (black) for 24 h. RNA was collected, reverse transcribed and analyzed by TaqMan for *mmp13* (B), *Sp7* (C) and *RankL* (D) expression. Scale is expanded to the right for the RUNX2 KO cells. Data are displayed as Relative Quantitation (RQ) normalized to *Gapdh* in a triplicate set of assays ± SEM. *, $p<0.05$ $1,25(OH)_2D_3$ versus vehicle within cell type by Student's t-test. a, $p<0.05$ basal vehicle of each line versus control by Student's t-test. E, Wildtype (WT, UAMS) or RUNX2 KO cells infected with pLeGO-G (control) or pLeGO-3xFLAG-OSX (F-OSX) were subjected to ChIP-qPCR analysis with antibodies to OSX, FLAG, and IgG using primers located at −30 kb, −20 kb, −10 kb, and the promoter proximal region (Pro) or F, *Vdr* U1, S1, or S3. WT + control is grey, WT + F-OSX is black, RUNX2 KO + control is red, and RUNX2 KO + F-OSX is green. Data are displayed as Quantity normalized to Input in triplicate ± SEM. *, $p<0.05$ F-OSX versus control within cell type and antibody by Student's t-test.

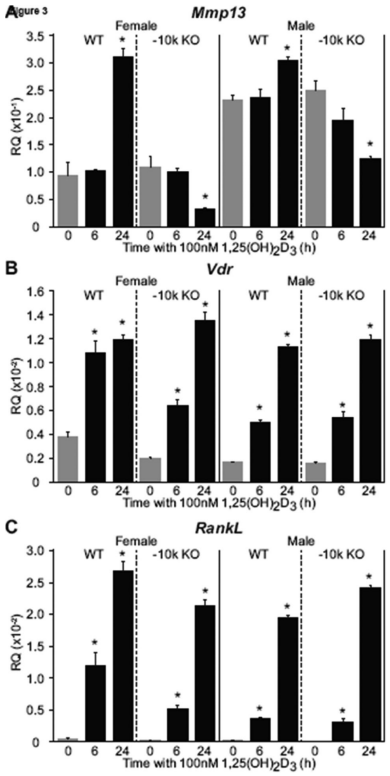

Figure 3.

In vivo enhancer deletion in mice reveals the loss of *mmp13* induction. Primary bone marrow cells were extracted from 2 month old mouse femur shafts of wildtype (WT) and −10 kb enhancer mice (−10k KO) male and female mice (n=3), cultured for 8 days and treated with 100 nM $1,25(OH)_2D_3$ for 0, 6, or 24 hours. RNA was extracted, reverse transcribed and analyzed by TaqMan for *mmp13* (A), *Vdr* (B), and *RankL* (C). Data are displayed as Relative Quantitation (RQ) normalized to *Gapdh* in a triplicate set of assays ± SEM. *, $p<0.05$ 24 h versus 0 h within mouse by Student's t-test.